A dual-reciprocity boundary element approach for axisymmetric nonlinear time-dependent heat conduction in a nonhomogeneous solid

B. I. Yun and W. T. Ang*
Division of Engineering Mechanics
School of Mechanical and Aerospace Engineering
Nanyang Technological University
50 Nanyang Avenue, Singapore 639798

Abstract

A dual-reciprocity boundary element method is presented for the numerical solution of a non-steady axisymmetric heat conduction problem involving a nonhomogeneous solid with temperature dependent properties. It is applied to solve some specific problems including one which involves the laser heating of a cylindrical solid.

Keywords: axisymmetric heat conduction, temperature-dependent material properties, boundary element method, dual-reciprocity method.

This paper will appear in *Engineering Analysis with Boundary Elements* (http://dx.doi.org/10.1016/j.enganabound.2010.03.013)

* Author for correspondence (W. T. Ang)
E-mail: mwtang@ntu.edu.sg
http://www.ntu.edu.sg/home/mwtang/

1 Introduction

Thermal conductivity and specific heat capacity of metallic solids have been experimentally observed to be strongly dependent on temperature during processes such as metal quenching. Thus, the development of numerical techniques for nonlinear heat conduction in solids with temperature dependent material properties has attracted the attention of many researchers in computational heat transfer. Earlier works on boundary element methods, such as Kikuta, Togoh and Tanaka [12] and Goto and Suzuki [9], assume that the solids are thermally isotropic and have density, specific heat capacity and thermal conductivity which are functions of temperature alone. Clements and Budhi [8], Azis and Clements [5] and, more recently, Ang and Clements [2] have proposed boundary element procedures for thermally anisotropic solids with material properties that vary with temperature and spatial coordinates.

The works in [2] and [5] are also applicable to linear heat conduction in nonhomogeneous media such as functionally graded materials. The analysis of functionally graded materials is a topic of special interest in boundary element methods. Some papers on boundary element methods for solving linear problems involving nonhomogeneous media with properties that vary continuously in space include Ang, Kusuma and Clements [3], Clements [7], Kassab and Divo [11], Park and Ang [16], Rangogni [17], Tanaka, Matsumoto and Suda [18] and other relevant references therein.

The present paper considers a nonlinear time-dependent axisymmetric heat conduction problem involving a nonhomogeneous thermally isotropic solid with temperature dependent properties. Such a problem is of practical interest as axisymmetric structures can be found in many engineering applications (such as pressure vessels and piping components). The analyses in Ang and Clements [2], Azis and Clements [5] and Brebbia, Telles and Wrobel [6] are used as a guide to convert the nonlinear partial differential equation governing the axisymmetric heat conduction into a suitable integro-differential equation. In addition to a boundary integral over a curve on an appropriate coordinate plane, the integro-differential equation also contains a domain integral. The dual-reciprocity approach is used here to express the domain integral approximately in terms of line integrals. The time derivative

of the temperature in the integro-differential formulation is approximated using a finite difference formula. At any given time level, if the temperature is assumed known at earlier time levels, the problem under consideration is formulated in terms of a system of nonlinear algebraic equations to be solved using a predictor-corrector (iterative) procedure.

The numerical procedure presented here is applied to solve some specific problems including one which involves the laser heating of a cylindrical solid. For problems which have known exact solutions, the accuracy of the numerical solutions obtained is assessed.

2 The problem

Consider a thermally isotropic solid occupying the three-dimensional region R. If T is the temperature inside the solid, then the conservation of energy and the classical Fourier's law of heat conduction require the temperature to satisfy the partial differential equation

$$\nabla \bullet (\kappa \nabla T) + Q = \rho c \frac{\partial T}{\partial t} \text{ in } R \text{ for } t \geq 0, \tag{1}$$

where ∇ is the gradient (nabla) operator, $\bullet$ denotes the dot product, t is time, ρ, c and κ are respectively the density, specific heat capacity and thermal conductivity of the solid and Q is the internal heat source generation rate.

With reference to a Cartesian coordinate system denoted by $Oxyz$, the geometry of the region R is symmetrical about the z-axis, that is, the boundary of R can be obtained by rotating a curve on the Oxz plane by an angle of 360^{o} about the z-axis. Furthermore, if r and θ denote the polar coodinates defined by $x = r\cos\theta$ and $y = r\sin\theta$, the temperature and the internal heat source generation rate are assumed to be independent of θ, given by $T(r, z, t)$ and $Q(r, z, t)$ respectively. The thermal conductivity is functionally graded in the radial and axial directions of the solid of revolution and is taken to be temperature dependent, such that

$$\kappa = g(r, z)h(T), \tag{2}$$

where g is a suitably given function which is positive in R and $h(T)$ is a function which is integrable with respect to T. The density ρ and the specific heat capacity c are also dependent on r, z and T.

Mathematically, the problem of interest here is to solve (1) together with (2) subject to the initial-boundary conditions

$$\begin{aligned} T(r,z,0) &= f_0(r,z) \text{ in } R, \\ T(r,z,t) &= f_1(r,z,t) \text{ on } S_1 \text{ for } t>0, \\ g(r,z)h(T)\frac{\partial T}{\partial n} &= f_2(r,z,t) \text{ on } S_2 \text{ for } t>0, \end{aligned} \tag{3}$$

where S_1 and S_2 are non-intersecting surfaces such that $S_1 \cup S_2 = S$, S is the (surface) boundary of the region R, $\partial T/\partial n$ denotes the outward normal derivative of T on S and $f_0(r,z)$, $f_1(r,z,t)$ and $f_2(r,z,t)$ are suitably given functions.

3 Transformed equations

Through the use of the Kirchhoff's transformation, that is,

$$\Theta(r,z,t) = \int h(T)dT \equiv \mathcal{K}(T) \tag{4}$$

the nonlinear governing partial differential equation defined by (1) and (2) can be rewritten as

$$g\nabla^2\Theta = -Q - \nabla g \bullet (\nabla\Theta) + S(r,z,\Theta)\frac{\partial\Theta}{\partial t}, \tag{5}$$

where

$$S(r,z,\Theta) = \frac{\rho(r,z,\mathcal{M}(\Theta))c(r,z,\mathcal{M}(\Theta))}{h(\mathcal{M}(\Theta))}, \tag{6}$$

if one assumes that (4) can be inverted to give the temperature as $T = \mathcal{K}^{-1}(\Theta) = \mathcal{M}(\Theta)$.

Furthermore, with the substitution

$$\Theta = \frac{1}{\sqrt{g}}\psi, \tag{7}$$

(5) becomes

$$\nabla^2\psi = -\frac{Q}{\sqrt{g}} + B(r,z)\psi + D(r,z,\psi)\frac{\partial\psi}{\partial t}, \tag{8}$$

where ∇^2 is the Laplacian differential operator and

$$B(r,z) = \frac{1}{\sqrt{g(r,z)}}\nabla^2(\sqrt{g(r,z)}), \;\; D(r,z,\psi) = \frac{1}{g}S(r,z,\frac{1}{\sqrt{g}}\psi). \qquad (9)$$

The function g is assumed to be such that $\nabla^2(\sqrt{g})$ exists in the solution domain R.

As ψ is a function of r, z and t, equation (8) can be written out more explicitly as

$$\frac{\partial^2\psi}{\partial r^2} + \frac{1}{r}\frac{\partial\psi}{\partial r} + \frac{\partial^2\psi}{\partial z^2} = -\frac{Q(r,z,t)}{\sqrt{g(r,z)}} + B(r,z)\psi + D(r,z,\psi)\frac{\partial\psi}{\partial t}. \qquad (10)$$

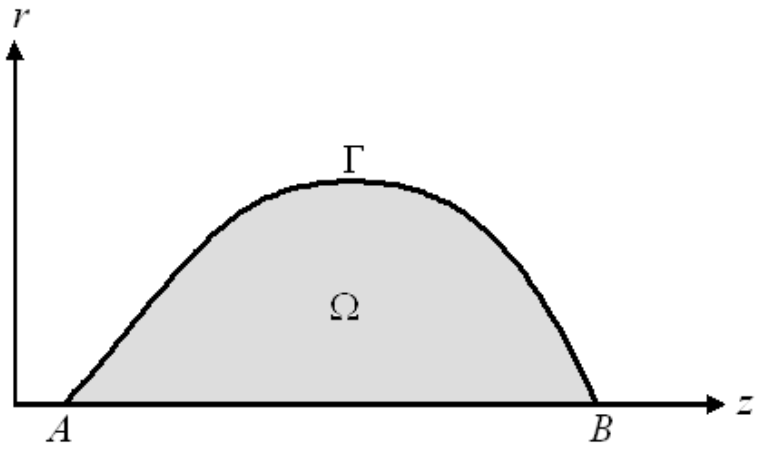

Figure 1. A sketch of Ω and Γ.

For the problem under consideration here, as pointed out earlier on in Section 2, the solution domain R and its boundary S can be obtained by rotating respectively a two-dimensional region and a curve by an angle of 360° about the z-axis. On the rz plane, the two-dimensional region and the curve are denoted by Ω and Γ respectively. Figure 1 gives a sketch of Ω (shaded region) and Γ. In Figure 1, Γ is an open curve having endpoints A and B on the z-axis. In general, Γ may also be a closed curve, as in,

for example, the case in which R is the hollow cylindrical region defined by $u < r < v$, $0 < z < w$, where u, v and w are positive constants.

In view of (4) and (7), the initial-boundary conditions in (3) can be rewritten on the rz plane as

$$\begin{aligned}
\psi(r,z,0) &= \sqrt{g(r,z)}\mathcal{K}(f_0(r,z)) \text{ in } \Omega, \\
\psi(r,z,t) &= \sqrt{g(r,z)}\mathcal{K}(f_1(r,z,t)) \text{ on } \Gamma_1 \text{ for } t>0, \\
\frac{\partial}{\partial n}[\psi(r,z,t)] &= \frac{\psi(r,z,t)}{2g(r,z)}\frac{\partial}{\partial n}[g(r,z)] + \frac{1}{\sqrt{g(r,z)}}f_2(r,z,t) \text{ on } \Gamma_2 \text{ for } t>0,
\end{aligned} \tag{11}$$

where Γ_1 and Γ_2 denote the curves that can be rotated by an angle of 360^o about the z-axis to generate the surfaces S_1 and S_2 respectively, and

$$\begin{aligned}
\frac{\partial}{\partial n}[\psi(r,z,t)] &= n_r(r,z)\frac{\partial}{\partial r}[\psi(r,z,t)] + n_z(r,z)\frac{\partial}{\partial z}[\psi(r,z,t)], \\
\frac{\partial}{\partial n}[g(r,z)] &= n_r(r,z)\frac{\partial}{\partial r}[g(r,z)] + n_z(r,z)\frac{\partial}{\partial z}[g(r,z)],
\end{aligned} \tag{12}$$

where $n_r(r,z)$ and $n_z(r,z)$ are the components of the outward unit normal vector on Γ at the point (r,z) in the r and z direction respectively.

Once $\psi(r,z,t)$ (hence $\Theta(r,z,t)$) is obtained by solving (10) in Ω subject to the initial-boundary conditions in (11), the temperature $T(r,z,t)$ may be obtained by inverting the Kirchhoff's transformation in (4).

4 Integro-differential formulation

An integro-differential equation in terms of integrals over Γ and Ω can be derived from (10), that is,

$$\begin{aligned}
&\gamma(r_0,z_0)\psi(r_0,z_0,t) \\
&= \iint_\Omega G_0(r,z;r_0,z_0)\{-\frac{Q(r,z,t)}{\sqrt{g(r,z)}} + B(r,z)\psi + D(r,z,\psi)\frac{\partial}{\partial t}[\psi(r,z,t)]\}rdrdz \\
&+ \int_\Gamma (\psi(r,z,t)G_1(r,z;r_0,z_0) - G_0(r,z;r_0,z_0)\frac{\partial}{\partial n}[\psi(r,z,t)])rds(r,z) \\
&\qquad \text{for } (r_0,z_0) \in \Omega \cup \Gamma,
\end{aligned} \tag{13}$$

where $\gamma(r_0, z_0) = 1$ if (r_0, z_0) lies in the interior of Ω, $\gamma(r_0, z_0) = 1/2$ if (r_0, z_0) lies on a smooth part of Γ, $ds(r, z)$ denotes the length of an infinitesimal part of the curve Γ, and

$$
\begin{aligned}
G_0(r, z; r_0, z_0) &= -\frac{K(m(r, z; r_0, z_0))}{\pi\sqrt{a(r, z; r_0, z_0) + b(r; r_0)}}, \\
G_1(r, z; r_0, z_0) &= -\frac{1}{\pi\sqrt{a(r, z; r_0, z_0) + b(r; r_0)}} \\
&\quad \times \{\frac{n_r(r, z)}{2r}[\frac{r_0^2 - r^2 + (z_0 - z)^2}{a(r, z; r_0, z_0) - b(r; r_0)} E(m(r, z; r_0, z_0)) \\
&\qquad - K(m(r, z; r_0, z_0))] \\
&\quad + n_z(r, z)\frac{z_0 - z}{a(r, z; r_0, z_0) - b(r; r_0)} E(m(r, z; r_0, z_0))\}, \\
m(r, z; r_0, z_0) &= \frac{2b(r; r_0)}{a(r, z; r_0, z_0) + b(r; r_0)}, \\
a(r, z; r_0, z_0) &= r_0^2 + r^2 + (z_0 - z)^2, \quad b(r; r_0) = 2rr_0,
\end{aligned} \tag{14}
$$

where K and E denote the complete elliptic integral of the first and second kind respectively. Note that $0 \leq m(r, z; r_0, z_0) \leq 1$ and K and E are as defined in Abramowitz and Stegun [1], that is,

$$
K(m) = \int_0^{\pi/2} \frac{d\theta}{\sqrt{1 - m\sin^2\theta}}, \quad E(m) = \int_0^{\pi/2} \sqrt{1 - m\sin^2\theta}\, d\theta. \tag{15}
$$

Some details on the derivation of (13) may be found in Brebbia, Telles and Wrobel [6].

Note that the integro-differential equation (13) does not involve any partial derivative of the unknown function with respect to the spatial coordinates r and z in its domain integral. If the integro-differential equation is derived directly by using (5) (instead of (10)) with Θ as an unknown function, the integrand of the domain integral will contain first order partial derivatives of Θ with respect to the spatial coordinates. The presence of those partial derivatives may be regarded as a disadvantage in the numerical solution of the integro-differential equation, as they have to be approximated in some way. Thus, the integro-differential equation in (13) is preferred over the one derived directly from (5) with unknown Θ.

5 Dual-reciprocity boundary element method

A dual-reciprocity boundary element method based on the integro-differential equation in (13) is described here for the approximate solution of the initial-boundary value problem defined by (10) and (11).

5.1 Boundary approximations

The curve Γ in Figure 1 is discretized into N straight line elements denoted by $\Gamma^{(1)}$, $\Gamma^{(2)}$, $\cdots$, $\Gamma^{(N-1)}$ and $\Gamma^{(N)}$. The starting and ending points of a typical element $\Gamma^{(k)}$ are given by $(r^{(k)}, z^{(k)})$ and $(r^{(k+1)}, z^{(k+1)})$ respectively. Two points on the element $\Gamma^{(k)}$, denoted by $(r_0^{(k)}, z_0^{(k)})$ and $(r_0^{(N+k)}, z_0^{(N+k)})$, are chosen as

$$\begin{aligned}(r_0^{(k)}, z_0^{(k)}) &= (r^{(k)}, z^{(k)}) + \tau(r^{(k+1)} - r^{(k)}, z^{(k+1)} - z^{(k)}),\\ (r_0^{(N+k)}, z_0^{(N+k)}) &= (r^{(k)}, z^{(k)}) + (1-\tau)(r^{(k+1)} - r^{(k)}, z^{(k+1)} - z^{(k)}),\end{aligned} \tag{16}$$

where τ is a chosen number such that $0 < \tau < 1/2$.

If the function ψ at $(r_0^{(k)}, z_0^{(k)})$ and $(r_0^{(N+k)}, z_0^{(N+k)})$ is denoted by $\psi^{(k)}(t)$ and $\psi^{(N+k)}(t)$ respectively, then the boundary temperature is approximated using

$$\psi(r,z,t) \simeq \frac{[s^{(k)}(r,z) - (1-\tau)\ell^{(k)}]\psi^{(k)}(t) - [s^{(k)}(r,z) - \tau\ell^{(k)}]\psi^{(N+k)}(t)}{(2\tau-1)\ell^{(k)}} \quad \text{for } (r,z) \in \Gamma^{(k)}, \tag{17}$$

where $\ell^{(k)} = s^{(k)}(r^{(k+1)}, z^{(k+1)})$ and $s^{(k)}(r,z)$ is the arc length along the element $\Gamma^{(k)}$ as defined by

$$s^{(k)}(r,z) = \sqrt{(r - r^{(k)})^2 + (z - z^{(k)})^2}. \tag{18}$$

Similarly, $q(r,z,t) = \partial\psi/\partial n$ is approximated using

$$q(r,z,t) \simeq \frac{[s^{(k)}(r,z) - (1-\tau)\ell^{(k)}]q^{(k)}(t) - [s^{(k)}(r,z) - \tau\ell^{(k)}]q^{(N+k)}(t)}{(2\tau-1)\ell^{(k)}} \quad \text{for } (r,z) \in \Gamma^{(k)}, \tag{19}$$

if $q^{(k)}(t) = q(r_0^{(k)}, z_0^{(k)}, t)$ and $q^{(N+k)}(t) = q(r_0^{(N+k)}, z_0^{(N+k)}, t)$.

Note that the approximations in (17) and (19) which are also used in Ang and Ooi [4] do not guarantee the continuity of $\psi(r, z, t)$ and $q(r, z, t)$ from one element to the next. They give rise to what are known as discontinuous linear elements in the literature (Paŕis and Cañas [15]).

With (17) and (19), the integro-differential equation (13) can be approximately written as

$$
\begin{aligned}
&\gamma(r_0, z_0)\psi(r_0, z_0, t) \\
&= \iint_{\Omega} G_0(r, z; r_0, z_0)\{-\frac{Q(r, z, t)}{\sqrt{g(r, z)}} + B(r, z)\psi + D(r, z, \psi)\frac{\partial}{\partial t}[\psi(r, z, t)]\}rdrdz \\
&+ \sum_{k=1}^{N} \frac{1}{(2\tau - 1)\ell^{(k)}}\{[-(1-\tau)\ell^{(k)}\mathcal{F}_2^{(k)}(r_0, z_0) + \mathcal{F}_4^{(k)}(r_0, z_0)]\psi^{(k)}(t) \\
&\qquad + [\tau\ell^{(k)}\mathcal{F}_2^{(k)}(r_0, z_0) - \mathcal{F}_4^{(k)}(r_0, z_0)]\psi^{(N+k)}(t) \\
&- [-(1-\tau)\ell^{(k)}\mathcal{F}_1^{(k)}(r_0, z_0) + \mathcal{F}_3^{(k)}(r_0, z_0)]q^{(k)}(t) \\
&\qquad - [\tau\ell^{(k)}\mathcal{F}_1^{(k)}(r_0, z_0) - \mathcal{F}_3^{(k)}(r_0, z_0)]q^{(N+k)}(t)\}, \qquad (20)
\end{aligned}
$$

where

$$
\begin{aligned}
\mathcal{F}_1^{(k)}(r_0, z_0) &= \int_{\Gamma^{(k)}} G_0(r, z; r_0, z_0)rds(r, z), \\
\mathcal{F}_2^{(k)}(r_0, z_0) &= \int_{\Gamma^{(k)}} G_1(r, z; r_0, z_0)rds(r, z), \\
\mathcal{F}_3^{(k)}(r_0, z_0) &= \int_{\Gamma^{(k)}} s(r, z)G_0(r, z; r_0, z_0)rds(r, z), \qquad (21) \\
\mathcal{F}_4^{(k)}(r_0, z_0) &= \int_{\Gamma^{(k)}} s(r, z)G_1(r, z; r_0, z_0)rds(r, z).
\end{aligned}
$$

The integrals over $\Gamma^{(k)}$ in (21) can be evaluated using numerically such as a highly accurate Gaussian quadrature.

5.2 Treatment of the domain integral

To treat the integral over the domain Ω in (20) using the dual-reciprocity method, L well-spaced out collocation points are chosen in the interior of the domain Ω. These points are denoted by $(r_0^{(2N+1)}, z_0^{(2N+1)})$, $(r_0^{(2N+2)}, z_0^{(2N+2)})$, $\cdots$, $(r_0^{(2N+L-1)}, z_0^{(2N+L-1)})$ and $(r_0^{(2N+L)}, z_0^{(2N+L)})$. The points $(r_0^{(k)}, z_0^{(k)})$ and $(r_0^{(N+k)}, z_0^{(N+k)})$ on the element $\Gamma^{(k)}$ $(k = 1, 2, \cdots, N)$, as defined in (16), are also used as collocation points.

According to Wang, Mattheij and ter Morsche [19], if one makes the approximation

$$\begin{aligned} & -\frac{Q(r,z,t)}{\sqrt{g(r,z)}} + B(r,z)\psi + D(r,z,\psi)\frac{\partial}{\partial t}[\psi(r,z,t)] \\ \simeq & \sum_{j=1}^{2N+L} \phi^{(j)}(r,z) \sum_{k=1}^{2N+L} W^{(kj)}\{-\frac{Q(r_0^{(k)}, z_0^{(k)}, t)}{\sqrt{g(r_0^{(k)}, z_0^{(k)})}} + B(r_0^{(k)}, z_0^{(k)})\psi^{(k)}(t) \\ & + D(r_0^{(k)}, z_0^{(k)}, \psi^{(k)}(t))\frac{d}{dt}[\psi^{(k)}(t)]\}, \end{aligned} \tag{22}$$

the domain integral may be approximately given by

$$\begin{aligned} & \iint_{\Omega} G_0(r,z;r_0,z_0)\{-\frac{Q(r,z,t)}{\sqrt{g(r,z)}} + B(r,z)\psi + D(r,z,\psi)\frac{\partial}{\partial t}[\psi(r,z,t)]\}rdrdz \\ \simeq & \sum_{k=1}^{2N+L}\{-\frac{Q(r_0^{(k)}, z_0^{(k)}, t)}{\sqrt{g(r_0^{(k)}, z_0^{(k)})}} + B(r_0^{(k)}, z_0^{(k)})\psi^{(k)}(t) \\ & + D(r_0^{(k)}, z_0^{(k)}, \psi^{(k)}(t))\frac{d}{dt}[\psi^{(k)}(t)]\} \sum_{j=1}^{2N+L} W^{(kj)}\Psi^{(j)}(r_0, z_0), \end{aligned} \tag{23}$$

where $\psi^{(k)}(t) = \psi(r_0^{(k)}, z_0^{(k)}, t)$ for $k = 1, 2, \cdots, 2N+L$, the coefficients $W^{(kj)}$ are defined implicitly by

$$\sum_{j=1}^{2N+L} W^{(kj)}\phi^{(p)}(r_0^{(j)}, z_0^{(j)}) = \begin{cases} 0 & \text{if} \quad p \neq k \\ 1 & \text{if} \quad p = k \end{cases} \quad \text{for } p,\ k = 1, 2, \cdots, 2N+L, \tag{24}$$

the functions $\Psi^{(j)}(r_0, z_0)$ are expressed in terms of line integrals over Γ as

$$\Psi^{(j)}(r_0, z_0) = \gamma(r_0, z_0)\chi^{(j)}(r_0, z_0) + \int_\Gamma rG_0(r, z; r_0, z_0)\frac{\partial}{\partial n}[\chi^{(j)}(r, z)]ds(r, z)$$
$$- \int_\Gamma r\chi^{(j)}(r, z)G_1(r, z; r_0, z_0)ds(r, z)$$
$$\text{for } j = 1, 2, \cdots, 2N + L, \tag{25}$$

the functions $\phi^{(p)}$ and $\chi^{(p)}$ may be constructed using

$$\phi^{(p)}(r, z) = \int_0^{2\pi} \nu(\sigma(r, \theta, z; r_0^{(p)}, z_0^{(p)}))d\theta, \quad \chi^{(p)}(r, z) = \int_0^{2\pi} \omega(\sigma(r, \theta, z; r_0^{(p)}, z_0^{(p)}))d\theta, \tag{26}$$

the function $\sigma(r, \theta, z; r_0^{(p)}, z_0^{(p)})$ is defined by

$$\sigma(r, \theta, z; r_0^{(p)}, z_0^{(p)}) = \sqrt{(r\cos\theta - r_0^{(p)})^2 + r^2\sin^2\theta + (z - z_0^{(p)})^2}, \tag{27}$$

and $\nu(\sigma(r, \theta, z; r_0^{(p)}, z_0^{(p)}))$ and $\omega(\sigma(r, \theta, z; r_0^{(p)}, z_0^{(p)}))$ are related to each other by

$$\nabla^2\omega(\sigma(r, \theta, z; r_0^{(p)}, z_0^{(p)})) = \nu(\sigma(r, \theta, z; r_0^{(p)}, z_0^{(p)})). \tag{28}$$

In Wang, Mattheij and ter Morsche [19], the functions $\nu(\sigma(r, \theta, z; r_0^{(p)}, z_0^{(p)}))$ and $\omega(\sigma(r, \theta, z; r_0^{(p)}, z_0^{(p)}))$ are chosen to be

$$\begin{aligned} \nu(\sigma(r, \theta, z; r_0^{(p)}, z_0^{(p)})) &= \sigma(r, \theta, z; r_0^{(p)}, z_0^{(p)}), \\ \omega(\sigma(r, \theta, z; r_0^{(p)}, z_0^{(p)})) &= \frac{1}{12}[\sigma(r, \theta, z; r_0^{(p)}, z_0^{(p)})]^3. \end{aligned} \tag{29}$$

From (26) together with (15) and

$$\int_0^{2\pi} (1 - m\sin^2(t))^{3/2}dt = \frac{1}{3}\begin{cases} 4(-1+m)K(m) + 8(2-m)E(m) \\ \qquad\qquad \text{if } 0 \le\ m < 1, \\ 8 \text{ if } m = 1, \end{cases} \tag{30}$$

the choice of $\nu(\sigma(r,\theta,z;r_0^{(p)},z_0^{(p)}))$ and $\omega(\sigma(r,\theta,z;r_0^{(p)},z_0^{(p)}))$ in (29) gives rise to

$$\begin{aligned}
\phi^{(p)}(r,z) &= 4\sqrt{a(r,z;r_0^{(p)},z_0^{(p)})+b(r;r_0^{(p)})}E(m(r,z;r_0^{(p)},z_0^{(p)})),\\
\chi^{(p)}(r,z) &= \frac{1}{9}[a(r,z;r_0^{(p)},z_0^{(p)})+b(r;r_0^{(p)})]^{3/2}\\
&\quad\times\begin{cases}(m(r,z;r_0^{(p)},z_0^{(p)})-1)K(m(r,z;r_0^{(p)},z_0^{(p)})\\ +[4-2m(r,z;r_0^{(p)},z_0^{(p)})]E(m(r,z;r_0^{(p)},z_0^{(p)}))\\ \qquad\qquad \text{if } 0\le\ m(r,z;r_0^{(p)},z_0^{(p)})<1,\\ 2 \text{ if } m(r,z;r_0^{(p)},z_0^{(p)})=1.\end{cases}
\end{aligned}\tag{31}$$

The first order partial derivatives of the function $\chi^{(p)}(r,z)$ in (31), as required in the evaluation of the first line integral on the right hand side of (25), can be obtained from (31) together with the results (see, for example, Whittaker and Watson [20])

$$\frac{d}{dm}(K(m))=\frac{1}{2m}(\frac{E(m)}{1-m}-K(m)),\quad \frac{d}{dm}(E(m))=\frac{1}{2m}(E(m)-K(m)).\tag{32}$$

The functions $\phi^{(p)}(r,z)$ and $\chi^{(p)}(r,z)$ are chosen to satisfy the partial differential equation

$$\frac{\partial^2\chi^{(p)}}{\partial r^2}+\frac{1}{r}\frac{\partial\chi^{(p)}}{\partial r}+\frac{\partial^2\chi^{(p)}}{\partial z^2}=\phi^{(p)}.\tag{33}$$

The choice of $\phi^{(p)}(r,z)$ and $\chi^{(p)}(r,z)$ is not unique. As constructed by using (26) and (28) together with (29), they are quite complicated in form, being expressed in terms of special functions, such as given in (31) where elliptic integrals are involved.

In earlier works on the axisymmetric dual-reciprocity boundary element method, such as Patridge, Brebbia and Wrobel [14], the approach is to choose $\chi^{(p)}(r,z)$ as a simple function of the distance between the field point (r,z) and the collocation point $(r_0^{(p)},z_0^{(p)})$ and determine the function $\phi^{(p)}(r,z)$ from (33). For example, if $\chi^{(p)}(r,z)$ is chosen as

$$\chi^{(p)}(r,z)=\frac{1}{9}[\sigma(r,0,z;r_0^{(p)},z_0^{(p)})]^3,\tag{34}$$

where $\sigma(r,0,z;r_0^{(p)},z_0^{(p)})$ is the distance between the points (r,z) and $(r_0^{(p)},z_0^{(p)})$ on the rz plane, that is,

$$\sigma(r,0,z;r_0^{(p)},z_0^{(p)}) = \sqrt{(r-r_0^{(p)})^2+(z-z_0^{(p)})^2}, \tag{35}$$

then $\phi^{(p)}(r,z)$ is given by

$$\phi^{(p)}(r,z) = [\frac{4}{3} - \frac{r_0^{(p)}}{3r}]\sigma(r,0,z;r_0^{(p)},z_0^{(p)}), \tag{36}$$

Although the interpolating function $\phi^{(p)}(r,z)$ constructed in this manner is simple in form (compared to (31)), its magnitude tends to infinity as $r \to 0$. Thus, if a certain part of the boundary of the domain Ω lies on the z axis (where $r = 0$), the use of (36) may compromise the accuracy of the approximation in (22).

Now if the function $\chi^{(p)}(r,z)$ can be chosen in such a way that the second term on the left hand side of (33) (that is, $r^{-1}\partial\chi^{(p)}/\partial r$) tends to a finite number as r tends to zero then $\phi^{(p)}(r,z)$ which is bounded in Ω can be constructed. To do this, a method which takes into consideration the virtual mirror image of the collocation point $(r_0^{(p)},z_0^{(p)})$ about the z axis (that is, the point $(-r_0^{(p)},z_0^{(p)})$) is proposed here. Specifically, we propose here to modify $\chi^{(p)}(r,z)$ in (34) to take the form

$$\chi^{(p)}(r,z) = \frac{1}{9}\{[\sigma(r,0,z;r_0^{(p)},z_0^{(p)})]^3 + [\sigma(r,0,z;-r_0^{(p)},z_0^{(p)})]^3\}. \tag{37}$$

The function $\phi^{(p)}(r,z)$ corresponding to $\chi^{(p)}(r,z)$ in (37) is then given by

$$\phi^{(p)}(r,z) = [\frac{4}{3} - \frac{r_0^{(p)}}{3r}]\sigma(r,0,z;r_0^{(p)},z_0^{(p)}) + [\frac{4}{3} + \frac{r_0^{(p)}}{3r}]\sigma(r,0,z;-r_0^{(p)},z_0^{(p)}). \tag{38}$$

One may easily check that the function $\phi^{(p)}(r,z)$ in (38) tends to a finite number as $r \to 0$.

Like (31), (38) gives $\phi^{(p)}(r,z)$ which is not partially differentiable with respect to r or z at $(r_0^{(p)},z_0^{(p)})$. The use of $\phi^{(p)}(r,z)$ given by either (31) or (38) however does not pose any difficulty for the problem here. This is because the left hand side of (22) does not contain any partial derivative of

the unknown function ψ with respect to r or z (hence the approximation of the domain integral as outlined in (23) does not involve any partial derivative of $\phi^{(p)}(r,z)$). If spatial derivatives of the unknown function are present in the domain integral then interpolating functions which are partially differentiable in Ω are needed in the dual-reciprocity method. It should be obvious now why it is advantageous to use the substitution in (7) in formulating the problem.

5.3 Time-stepping and iterative procedure

Approximating $\psi^{(k)}(t)$ and its first order derivative by

$$\begin{aligned} \psi^{(k)}(t) &\simeq \frac{1}{2}[\psi^{(k)}(t+\frac{1}{2}\Delta t)+\psi^{(k)}(t-\frac{1}{2}\Delta t)], \\ \frac{d}{dt}[\psi^{(k)}(t)] &\simeq \frac{\psi^{(k)}(t+\frac{1}{2}\Delta t)-\psi^{(k)}(t-\frac{1}{2}\Delta t)}{\Delta t}, \end{aligned} \tag{39}$$

and letting (r_0,z_0) in (20) be given in turn by $(r_0^{(1)},z_0^{(1)})$, $(r_0^{(2)},z_0^{(2)})$, $\cdots$, $(r_0^{(2N+L-1)},z_0^{(2N+L-1)})$ and $(r_0^{(2N+L)},z_0^{(2N+L)})$, one finds that (20) and (23) give

$$\begin{aligned} &\frac{1}{2}\gamma(r_0^{(m)},z_0^{(m)})[\psi^{(m)}(t+\frac{1}{2}\Delta t)+\psi^{(m)}(t-\frac{1}{2}\Delta t)] \\ &= \sum_{k=1}^{2N+L}\{-\frac{Q(r_0^{(k)},z_0^{(k)},t)}{\sqrt{g(r_0^{(k)},z_0^{(k)})}}+B(r_0^{(k)},z_0^{(k)})\psi^{(k)}(t) \\ &+ F^{(k)}(t)\frac{\psi^{(k)}(t+\frac{1}{2}\Delta t)-\psi^{(k)}(t-\frac{1}{2}\Delta t)}{\Delta t}\}\mu^{(km)} \\ &+ \sum_{k=1}^{N}\frac{1}{(2\tau-1)\ell^{(k)}}\{[-(1-\tau)\ell^{(k)}\mathcal{F}_2^{(k)}(r_0^{(m)},z_0^{(m)}) \\ &\qquad + \mathcal{F}_4^{(k)}(r_0^{(m)},z_0^{(m)})]\psi^{(k)}(t) \\ &\quad + [\tau\ell^{(k)}\mathcal{F}_2^{(k)}(r_0^{(m)},z_0^{(m)})-\mathcal{F}_4^{(k)}(r_0^{(m)},z_0^{(m)})]\psi^{(N+k)}(t) \\ &- [-(1-\tau)\ell^{(k)}\mathcal{F}_1^{(k)}(r_0^{(m)},z_0^{(m)})+\mathcal{F}_3^{(k)}(r_0^{(m)},z_0^{(m)})]q^{(k)}(t) \\ &\quad - [\tau\ell^{(k)}\mathcal{F}_1^{(k)}(r_0^{(m)},z_0^{(m)})-\mathcal{F}_3^{(k)}(r_0^{(m)},z_0^{(m)})]q^{(N+k)}(t)\} \\ &\qquad\qquad \text{for } m=1,2,\cdots,2N+L, \end{aligned} \tag{40}$$

where

$$F^{(k)}(t) = D(r_0^{(k)}, z_0^{(k)}, \psi^{(k)}(t)),\ \mu^{(km)} = \sum_{j=1}^{2N+L} W^{(kj)}\Psi^{(j)}(r_0^{(m)}, z_0^{(m)}). \qquad (41)$$

Application of the boundary conditions on the second and third lines of (11) into (40) yields

$$\begin{aligned}
&\gamma(r_0^{(m)}, z_0^{(m)})\{\frac{\alpha^{(m)}}{2}[\psi^{(m)}(t+\frac{1}{2}\Delta t) + \psi^{(m)}(t-\frac{1}{2}\Delta t)] + \beta^{(m)}R^{(m)}(t)\} \\
&= \sum_{k=1}^{2N+L}\{B(r_0^{(k)}, z_0^{(k)})(\frac{\alpha^{(k)}}{2}[\psi^{(k)}(t+\frac{1}{2}\Delta t) + \psi^{(k)}(t-\frac{1}{2}\Delta t)] + \beta^{(k)}R^{(k)}(t)) \\
&+ F^{(k)}(t)(\alpha^{(k)}\frac{\psi^{(k)}(t+\frac{1}{2}\Delta t) - \psi^{(k)}(t-\frac{1}{2}\Delta t)}{\Delta t} \\
&\qquad + \beta^{(k)}\frac{d}{dt}[R^{(k)}(t)]) - \frac{Q(r_0^{(k)}, z_0^{(k)}, t)}{\sqrt{g(r_0^{(k)}, z_0^{(k)})}}\}\mu^{(km)} \\
&+ \sum_{k=1}^{N}\frac{1}{(2\tau-1)\ell^{(k)}}\{[-(1-\tau)\ell^{(k)}\mathcal{F}_2^{(k)}(r_0^{(m)}, z_0^{(m)}) + \mathcal{F}_4^{(k)}(r_0^{(m)}, z_0^{(m)}) \\
&\qquad - \alpha^{(k)}Z^{(k)}(t)(-(1-\tau)\ell^{(k)}\mathcal{F}_1^{(k)}(r_0^{(m)}, z_0^{(m)}) + \mathcal{F}_3^{(k)}(r_0^{(m)}, z_0^{(m)}))] \\
&\quad \times (\frac{\alpha^{(k)}}{2}[\psi^{(k)}(t+\frac{1}{2}\Delta t) + \psi^{(k)}(t-\frac{1}{2}\Delta t)] + \beta^{(k)}R^{(k)}(t)) \\
&\quad + [\tau\ell^{(k)}\mathcal{F}_2^{(k)}(r_0^{(m)}, z_0^{(m)}) - \mathcal{F}_4^{(k)}(r_0^{(m)}, z_0^{(m)}) \\
&\quad - \alpha^{(N+k)}Z^{(N+k)}(t)(\tau\ell^{(k)}\mathcal{F}_1^{(k)}(r_0^{(m)}, z_0^{(m)}) - \mathcal{F}_3^{(k)}(r_0^{(m)}, z_0^{(m)}))] \\
&\quad \times (\frac{\alpha^{(N+k)}}{2}[\psi^{(N+k)}(t+\frac{1}{2}\Delta t) + \psi^{(N+k)}(t-\frac{1}{2}\Delta t)] + \beta^{(N+k)}R^{(N+k)}(t)) \\
&\quad - [-(1-\tau)\ell^{(k)}\mathcal{F}_1^{(k)}(r_0^{(m)}, z_0^{(m)}) + \mathcal{F}_3^{(k)}(r_0^{(m)}, z_0^{(m)})] \\
&\qquad \times [\alpha^{(k)}Y^{(k)}(t) + \beta^{(k)}q^{(k)}(t)] \\
&\quad - [\tau\ell^{(k)}\mathcal{F}_1^{(k)}(r_0^{(m)}, z_0^{(m)}) - \mathcal{F}_3^{(k)}(r_0^{(m)}, z_0^{(m)})] \\
&\qquad \times [\alpha^{(N+k)}Y^{(N+k)}(t) + \beta^{(N+k)}q^{(N+k)}(t)]\} \\
&\qquad\qquad \text{for } m = 1, 2, \cdots, 2N+L, \qquad (42)
\end{aligned}$$

where $R^{(m)}(t)$, $\alpha^{(m)}$, $\beta^{(m)}$, $Y^{(p)}(t)$ and $Z^{(p)}(t)$ for $m = 1, 2, \cdots, 2N+L$ and

$p = 1, 2, \cdots, N, N+1, \cdots, 2N-1, 2N$ are defined by

$$
\begin{aligned}
R^{(m)}(t) &= \sqrt{g(r_0^{(m)}, z_0^{(m)})}\mathcal{K}(f_1(r_0^{(m)}, z_0^{(m)}, t)), \\
\alpha^{(m)} &= \begin{cases} 0 & \text{if } (r_0^{(m)}, z_0^{(m)}) \text{ lies on a boundary element} \\ & \text{where } \psi \text{ is specified,} \\ 1 & \text{otherwise,} \end{cases} \\
\beta^{(m)} &= 1 - \alpha^{(m)}, \\
Y^{(p)}(t) &= \frac{1}{\sqrt{g(r_0^{(p)}, z_0^{(p)})}} f_2(r_0^{(p)}, z_0^{(p)}, t), \\
Z^{(p)}(t) &= \frac{1}{2g(r_0^{(p)}, z_0^{(p)})}(n_r(r,z)\frac{\partial}{\partial r}[g(r,z)] \\
&\qquad + n_z(r,z)\frac{\partial}{\partial z}[g(r,z)])\Big|_{(r,z)=(r_0^{(p)}, z_0^{(p)})}. \qquad (43)
\end{aligned}
$$

Note that $[n_r(r_0^{(p)}, z_0^{(p)}), n_z(r_0^{(p)}, z_0^{(p)})]$ gives the outward unit normal vector to the boundary element which contains the collocation point $(r_0^{(p)}, z_0^{(p)})$. Thus, $[n_r(r_0^{(k)}, z_0^{(k)}), n_z(r_0^{(k)}, z_0^{(k)})]$ and $[n_r(r_0^{(N+k)}, z_0^{(N+k)}), n_z(r_0^{(N+k)}, z_0^{(N+k)})]$ both refer to the outward unit normal vector to the boundary element denoted by $\Gamma^{(k)}$. Also, note that $f_2(r_0^{(p)}, z_0^{(p)}, t)$ (hence $Y^{(p)}(t)$) is defined only if $(r_0^{(p)}, z_0^{(p)})$ is a collocation point on a boundary element where ψ is not specified. (In (42), $Y^{(p)}(t)$ is always multipled to $\alpha^{(p)}$. Hence, the calculation of $Y^{(p)}(t)$ is needed only if $(r_0^{(p)}, z_0^{(p)})$ is a collocation point on a boundary element where ψ is not specified.)

If $F^{(n)}(t)$ and $\psi^{(n)}(t - \frac{1}{2}\Delta t)$ are assumed known for $n = 1, 2, \cdots, 2N + L$ then (42) constitutes a system of $2N+L$ linear algebraic equations containing $2N + L$ unknowns. There are L unknowns at the interior collocation points as given by $\psi^{(p)}(t+\frac{1}{2}\Delta t)$ for $p = 2N+1, 2N+2, \cdots, 2N+L$. The remaining $2N$ unknowns are given either by $\psi^{(k)}(t + \frac{1}{2}\Delta t)$ and $\psi^{(N+k)}(t + \frac{1}{2}\Delta t)$ (if ψ is not specified on $\Gamma^{(k)}$) or $q^{(k)}(t)$ and $q^{(N+k)}(t)$ (if ψ is specified on $\Gamma^{(k)}$). The unknowns can be determined numerically by repeating the steps below until the numerical values of ψ at the selected points are obtained at the desired time level.

1. From the initial condition given in (11), compute the values of $\psi^{(n)}(0)$ for $n = 1, 2, \cdots, 2N + L$. Choose a small positive time-step Δt. Set the integer $J = 0$. Go to Step 2.

2. Estimate the values of $F^{(n)}((J + \frac{1}{2})\Delta t)$ using the latest known values of $\psi^{(n)}(J\Delta t)$, that is, $F^{(n)}((J+\frac{1}{2})\Delta t) \simeq D(r_0^{(n)}, z_0^{(n)}, \psi^{(n)}(J\Delta t))$. Go to Step 3.

3. Using the latest known values of $F^{(n)}((J + \frac{1}{2})\Delta t)$ and $\psi^{(n)}(J\Delta t)$, let $t = (J+\frac{1}{2})\Delta t$ in (42) to set up a system of linear algebraic equations and solve for the unknowns. The unknowns are given by $\psi^{(m)}((J + 1)\Delta t)$ for $m = 2N+1, 2N+2, \cdots, 2N+L$, and either by $\psi^{(k)}((J+1)\Delta t)$ and $\psi^{(N+k)}((J + 1)\Delta t)$ (if ψ is not specified on $\Gamma^{(k)}$) or by $q^{(k)}((J + \frac{1}{2})\Delta t)$ and $q^{(N+k)}((J + \frac{1}{2})\Delta t)$ (if ψ is specified on $\Gamma^{(k)}$) for $k = 1, 2, \cdots, N$. Go to Step 4.

4. Use the latest known values of $\psi^{(n)}((J+1)\Delta t)$ obtained in Step 3 above to compute $\psi^{(n)}((J+\frac{1}{2})\Delta t) = \frac{1}{2}[\psi^{(n)}((J+1)\Delta t)+\psi^{(n)}(J\Delta t)]$ for $n = 1, 2, \cdots, 2N + L$. Re-calculate $F^{(n)}((J + \frac{1}{2})\Delta t)$ using $F^{(n)}((J + \frac{1}{2})\Delta t) \simeq D(r_0^{(n)}, z_0^{(n)}, \psi^{(n)}((J+\frac{1}{2})\Delta t))$. Check whether the newly obtained values of $F^{(n)}((J + \frac{1}{2})\Delta t)$ agree with the previous values to within a specified number of significant figures. If the required convergence is not achieved, go to Step 3. Otherwise, increase the current value of J by 1 and go to Step 2.

6 Specific problems

The dual-reciprocity boundary element procedure described in Section 5 is applied here to solve some specific problems incuding one which involves the laser heating of a cylindrical solid.

For treating the domain integral, the relatively simple interpolating function $\phi^{(p)}(r, z)$ proposed in (38) is used in all the problems below. For Problems 1, 2 and 3 which have known exact solutions, we have also repeated all the calculations using the more complicated interpolating function $\phi^{(p)}(r, z)$ in (31) and found that the two interpolating functions deliver numerical solutions which are of comparable accuracy.

Problem 1. Take the solution domain $1 < r < 2$, $0 < z < 1$ (a hollow cylinder). The coefficients κ, ρ and c are given by $\kappa = 1 + r^2$ and $\rho c = 1$. The function Q is given by

$$Q = -\{\frac{21}{2}r^2 + \frac{1}{2}z^2 + 6\}\exp(-\frac{1}{2}t) - \frac{4}{r^4}.$$

The initial-boundary conditions are taken to be

$$\begin{aligned}
T(r,z,0) &= \frac{1}{r^2} + r^2 + z^2 \text{ for } 1 < r < 2, 0 < z < 1,\\
T(r,0,t) &= \frac{1}{r^2} + r^2\exp(-\frac{1}{2}t) \text{ for } 1 < r < 2 \text{ and } t > 0,\\
T(r,1,t) &= \frac{1}{r^2} + (r^2+1)\exp(-\frac{1}{2}t) \text{ for } 1 < r < 2 \text{ and } t > 0,\\
(1+r^2)\frac{\partial T}{\partial r}\Big|_{r=1} &= -4 + 4\exp(-\frac{1}{2}t) \text{ for } 0 < z < 1 \text{ and } t > 0,\\
(1+r^2)\frac{\partial T}{\partial r}\Big|_{r=2} &= -\frac{5}{4} + 20\exp(-\frac{1}{2}t) \text{ for } 0 < z < 1 \text{ and } t > 0.
\end{aligned}$$

For the problem here, the curve Γ in the integro-differential formulation is a closed one which comprises the four sides of the square region $1 < r < 2$, $0 < z < 1$, on the rz plane. To apply the dual-reciprocity boundary element method to solve the problem numerically, each of the sides is discretized into N_0 elements of equal length (so that $N = 4N_0$) and the M^2 interior collocation points are chosen to be given by $(r,z) = (1+i/(M+1), j/(M+1))$ for $i = 1, 2, \cdots, M$ and $j = 1, 2, \cdots, M$.

The governing partial differential equation is linear and T is related to ψ by $\psi = \sqrt{1+r^2}T$. Hence, for the problem here, at a given time level $t = (J + \frac{1}{2})\Delta t$, it is not necessary to iterate between Steps 3 and 4 (in the procedure outlined in Section 5).

Two sets of numerical values are obtained for T. The first set (Set A) is obtained by using $N_0 = 10$, $M = 3$ and $\Delta t = 0.30$, while the second set (Set B) by $N_0 = 20$, $M = 15$ and $\Delta t = 0.10$. In both sets, the parameter τ in the discontinuous linear elements is chosen to be 0.25. In Table 1, at selected interior points and time $t = 0.45$, the numerical values of T in Sets A and B are compared with the exact solution given by

$$T(r,z,t) = \frac{1}{r^2} + (r^2+z^2)\exp(-\frac{1}{2}t).$$

Both sets of numerical values of T are reasonably accurate. The percentage errors of the numerical values in Sets A and B are less than 0.25% and 0.09% respectively. It is obvious that the numerical values of T converge to the exact solution (that is, there is a significant improvement in the accuracy of the numerical values) when the calculation is refined by reducing the sizes of the boundary elements used, increasing the number of interior collocation points and decreasing the time-step.

Table 1. Numerical and exact values of T at selected interior points and time $t = 0.45$.

Point (r, z)	Set A	Set B	Exact
$(1.25, 0.25)$	1.93380	1.93744	1.93759
$(1.50, 0.25)$	2.28949	2.29095	2.29101
$(1.75, 0.25)$	2.82081	2.82186	2.82189
$(1.25, 0.50)$	2.08189	2.08711	2.08731
$(1.50, 0.50)$	2.43835	2.44064	2.44073
$(1.75, 0.50)$	2.96997	2.97156	2.97162
$(1.25, 0.75)$	2.33285	2.33671	2.33685
$(1.50, 0.75)$	2.68863	2.69022	2.69027
$(1.75, 0.75)$	3.21999	3.22113	3.22115

Problem 2. The solution domain is taken to be $0 < r < 1$, $0 < z < 1$ (a solid cylinder). The coefficients κ, ρ and c are given by $\kappa = (1+z)(1+T)$ and $\rho c = 1$ and the function Q is given by

$$Q(r, z, t) = \frac{(1+z)^2 - 2t - 4t^2 - 2zt - 2zt^2}{(1+z)^3 (1+t)^2}.$$

The initial-boundary conditions are taken to be

$$\begin{aligned} T(r, z, 0) &= 1 \text{ for } 0 < r < 1,\ 0 < z < 1, \\ T(r, 0, t) &= \frac{1+2t}{1+t} \text{ for } 0 < r < 1,\ t > 0, \\ T(r, 1, t) &= \frac{2+3t}{2(1+t)} \text{ for } 0 < r < 1,\ t > 0, \\ (1+z)(1+T) \left.\frac{\partial T}{\partial r}\right|_{r=1} &= 0 \text{ for } 0 < z < 1,\ t > 0. \end{aligned}$$

For the problem here, the curve Γ on the rz plane consists of three straight line segments of unit length. To apply the dual-reciprocity boundary element method to solve the problem numerically, each of these line segments is discretized into N_0 equal length boundary elements (so that $N = 3N_0$) and the M^2 interior collocation points are chosen to be given by $(r, z) = (i/(M+1), j/(M+1))$ for $i = 1, 2, \cdots, M$ and $j = 1, 2, \cdots, M$.

According to the Kirchoff's transformation, the function ψ may be taken to be related to T by $\psi = \sqrt{1+z}(T + \frac{1}{2}T^2)$. Here the governing partial differential equation in ψ is nonlinear with the coefficient $D(r, z, \psi)$ of $\partial\psi/\partial t$ being given by

$$D(r, z, \psi) = \frac{1}{(1+z)\sqrt{1 + 2\psi/\sqrt{1+z}}}.$$

At a given time level $t = (J+\frac{1}{2})\Delta t$, Steps 3 and 4 (in the numerical procedure outlined in Section 5) are iterated until the value of $F^{(n)}((J+\frac{1}{2})\Delta t)$ averaged over all the collocation points does not change by more than 0.001% from one iteration to the next. In the numerical results presented below, not more than 10 iterations are required in the calculation.

Table 2. Numerical and exact values of T at $(r, z) = (0.50, 0.50)$ and at selected time levels.

Time t	Set A	Set B	Exact
0.15	1.08398	1.08675	1.08696
0.45	1.20811	1.20683	1.20690
0.75	1.28491	1.28567	1.28571
1.05	1.34189	1.34145	1.34146
1.35	1.38269	1.38297	1.38298

As in Problem 1 above, two sets of numerical results are obtained for T. Sets A and B are obtained by using $(N_0, M, \Delta t) = (10, 7, 0.30)$ and $(N_0, M, \Delta t) = (20, 15, 0.10)$ respectively. In both sets, the parameter τ in the discontinuous linear elements is set to 0.25. In Table 2, the numerical

values of T at the point $(r, z) = (0.50, 0.50)$ are compared with the exact solution of the problem at various time levels. The exact solution is given by

$$T(r, z, t) = 1 + \frac{t}{(1+z)(1+t)}.$$

As may be expected, the numerical values of T in Set B are found to be more accurate than those in Set A. The percentage errors in the numerical values in Sets A and B are less than 0.3% and 0.02% respectively.

Problem 3. Take the solution domain Ω on the rz plane to be the region bounded by the lines $r = z$, $r = 0$ and $z = 1$. (Rotating Ω by an angle of 360° about the z axis gives rise to R which is a conical region.) The coefficients κ, ρ and c are given by $\kappa = T$ and $\rho c = T$. The function Q is given by

$$Q = (\frac{1}{2} - 2(r^2 + z^2)) \exp(-(t + r^2 - z^2)).$$

The initial-boundary conditions are taken to be

$$\begin{aligned} T(r, z, 0) &= \exp(-\frac{1}{2}(r^2 - z^2)) \text{ for } (r, z) \text{ in } R, \\ T(r, z, t) &= \exp(-\frac{t}{2}) \text{ on } r = z \text{ for } 0 < z < 1, \\ T\frac{\partial T}{\partial n} &= T - \exp(-\frac{1}{2}(t + r^2 - 1)) + \exp(-(t + r^2 - 1)) \\ &\quad \text{on } z = 1 \text{ for } 0 < r < 1 \text{ and } t > 0. \end{aligned}$$

For the problem under consideration here, with the transformation $\psi = \frac{1}{2}T^2$, the boundary condition involving the flux $\partial T/\partial n$ and temperature T (that is, the so called Robin condition) can be rewritten as

$$\begin{aligned} \frac{\partial \psi}{\partial n} &= \sqrt{2\psi} - \exp(-\frac{1}{2}(t + r^2 - 1)) + \exp(-(t + r^2 - 1)) \\ &\quad \text{on } z = 1 \text{ for } 0 < r < 1 \text{ and } t > 0. \end{aligned}$$

Unlike in (11), the above transformed boundary condition for the problem here contains a nonlinear term. The nonlinear term in the boundary condition can be treated as explained below.

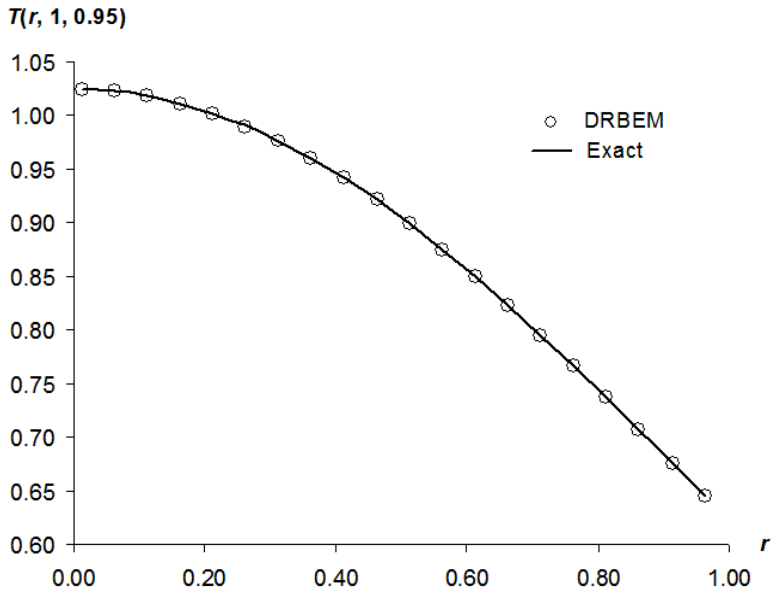

Figure 2. A graphical comparison of numerical and exact temperature on $z = 1$, $0 < r < 1$, at time $t = 0.95$.

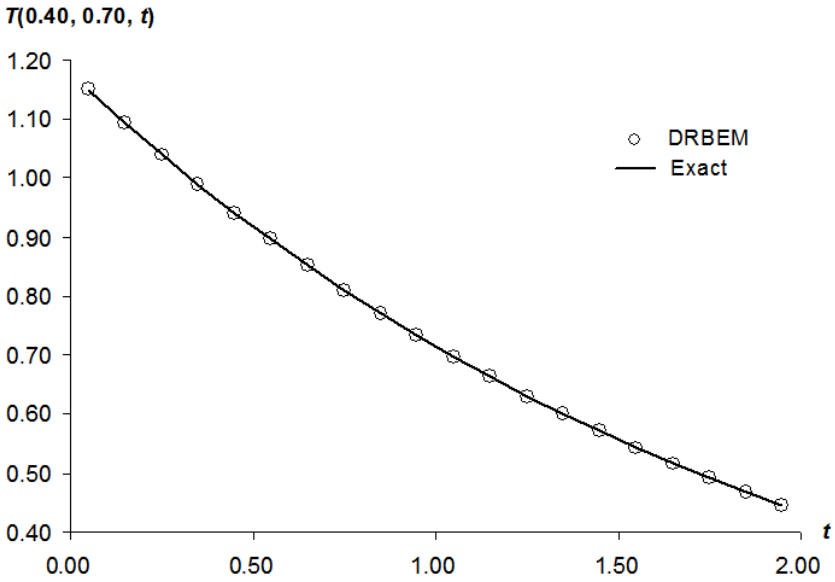

Figure 3. A graphical comparison of numerical and exact temperature at point $(r, z) = (0.40, 0.70)$ over the period $0 < t < 2$.

At a fixed time level $t = (J+\frac{1}{2})\Delta t$ ($J = 0, 1, 2, \cdots$), the nonlinear term in the transformed boundary condition is first approximated using the solution ψ at $t = J\Delta t$. The solution ψ at $t = (J+\frac{1}{2})\Delta t$ can then be obtained approximately by solving the linear algebraic equations in the boundary element procedure as explained in Section 5. The approximation of the nonlinear term in the boundary condition can be updated by using the just obtained solution ψ at $t = (J+\frac{1}{2})\Delta t$ and the boundary element procedure can be used again to solve for ψ at $t = (J + \frac{1}{2})\Delta t$. The process can be iterated until the temperature at the collocation points converges to within a specified number of significant figures.

To obtain some numerical results, the boundary Γ is discretized into 100 elements, the parameter τ in the discontinuous elements is taken to be 0.25, 36 well spaced points are selected as interior collocation points and the time-step Δt is chosen to be 0.10. Iteration on the nonlinear boundary condition is stopped when the temperature does not change by more than 0.001% at all the collocation points. Typically, not more than 10 iterations are required in the calculation. As the temperature is not known a priori on the boundary $z = 1$ ($0 < r < 1$), the numerical values of the boundary temperature there at $t = 0.95$ are compared graphically with the exact temperature $T(r, z, t) = \exp(-\frac{1}{2}(t + r^2 - z^2))$ in Figure 2. In Figure 3, the numerical and the exact values of T at the point $(r, z) = (0.40, 0.70)$ are plotted against time t for $0 < t < 2$. The numerical and exact temperature agree well with each other. The percentage errors of the numerical values in Figures 2 and 3 are less than 0.12% and 0.07% respectively.

Problem 4. Consider a cylindrical solid of radius a and height b. Specifically, the cylindrical solid occupies the region $0 < r < a$, $0 < z < b$. It is subject to laser heating on the surface $z = 0$. The laser heating may be modeled by taking

$$Q(r, z, t) = \phi(t)\mu(1 - R)I(r)\exp(-\mu z),$$

where μ is the laser absorption coefficient, R is the Fresnel surface reflectance, $\phi(t)$ is a given function controlling the laser heating and $I(r)$ is the incident irradiance at the center $(0, 0)$ on the surface $z = 0$. Specifically, $I(r)$ is chosen

here to take the Gaussian form

$$I(r) = I_0 \exp(-\frac{2r^2}{w^2}),$$

where I_0 is the peak irradiance and w is the radius of the laser beam. For some details of problems involving laser heating of solids, refer to, for example, Gutierrez and Jen [10] and Ooi, Ang and Ng [13].

The initial-boundary conditions are given by

$$\begin{aligned} T(r,z,0) &= T_0 \text{ for } (r,z) \text{ inside the solid,} \\ \kappa\frac{\partial T}{\partial n} &= 0 \text{ on } r = a \text{ for } t > 0, \\ \kappa\frac{\partial T}{\partial n} &= h_{\text{amb}}(T_{\text{amb}} - T) \text{ on } z = 0,\ 0 < r < a \text{ for } t > 0, \\ \kappa\frac{\partial T}{\partial n} &= 0 \text{ on } z = b,\ 0 < r < a \text{ for } t > 0, \end{aligned}$$

where T_0 is a given constant, h_{amb} is the ambient convection coefficient and T_{amb} is the ambient temperature.

As pointed out in [10], the high temperature gradient generated by the laser heating may result in significant changes in the thermal properties of the solid. The thermal conductivity κ and specific heat capacity c are modeled to vary with temperature in accordance with

$$\begin{aligned} \kappa &= \kappa_0 + \kappa_1(T - T_0), \\ c &= c_0 + c_1(T - T_0) + c_2(T - T_0)^2, \end{aligned}$$

where κ_0, κ_1, c_0, c_1 and c_2 are given constants.

For the purpose of obtaining some results, the material constants of polymethyl methacrylate (PMMA) are used here. They are given by $\rho = 1180$ kg/m^3, $\kappa_0 = 0.19$ W/(m K), $\kappa_1 = -0.19 \times 10^{-3}$ W/(m K^2), $c_0 = 1500$ J/(kg K), $c_1 = 4.5$ J/(kg K^2) and $c_2 = 0$ J/(kg K^3) (Gutierrez and Jen [10]). The laser absorption coefficient μ is 5.0×10^4 m^{-1}. The other laser parameters required in the heat generation term are taken to be $(1 - R)I_0 = 1.0 \times 10^5$ W/m^2, $w = 0.0003$ m and $\phi(t) = 1$ for $t \geq 0$. The initial temperature T_0, the ambient temperature T_{amb} and the ambient convection coefficient h_{amb} are 310 K, 300 K and 10 W/(m^2 K) respectively. The dimensions of the PMMA

cylinder are given by $a = b = 1$ mm. The calculation of the temperature is carried using 60 elements on the curve Γ and 441 collocation points in the interior of the solution domain. The time-step used is $\Delta t = 0.093$ s.

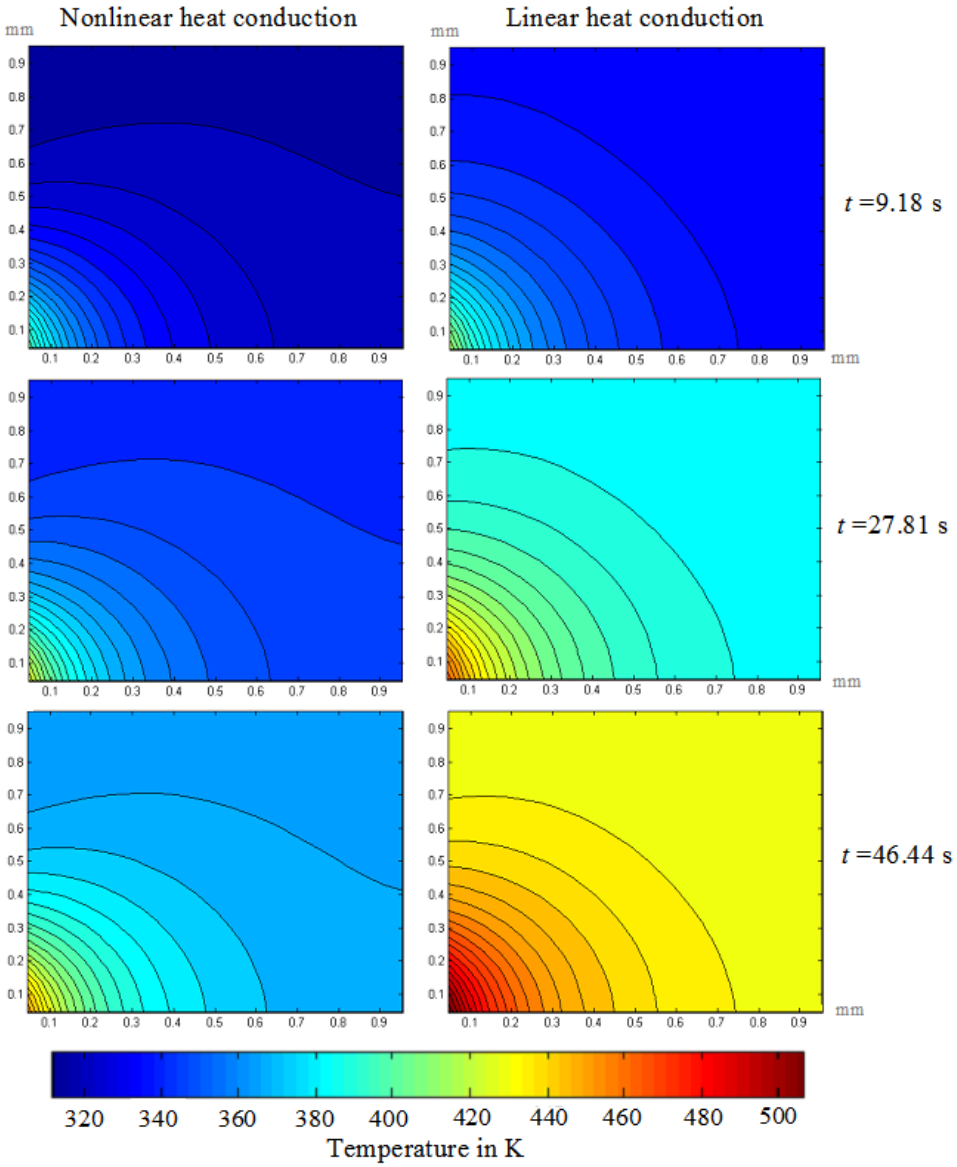

Figure 4. Spatial temperature profiles for nonlinear and linear heat conduction at selected time instants.

The spatial temperature profiles over the solution domain $0 < r < 1$ mm, $0 < z < 1$ mm, at selected time instants $t = 9.18$ s, $t = 27.81$ s and $t = 46.44$ s are depicted by the plots in Figure 4 (under "nonlinear heat conduction"). Figure 4 also shows the corresponding temperature profiles for linear heat conduction (obtained by using $\kappa_1 = 0$, $c_1 = 0$ and $c_2 = 0$). Due to continuous laser heating, the temperature increases with time, as expected. According to the linear theory of heat conduction, at time $t = 46.44$ s, the temperature in the solid ranges from about 420 K (in most part) to a maximum of over 500 K (at the center of heating). At the same time instant, the temperature given by the nonlinear theory is only around 440 K very close to the center of heating and is below 400 K in most part of the solid. Thus, it appears that linear theory predicts a quicker heating up of the solid than the nonlinear one.

To investigate further the effects of the temperature-dependent terms in the thermal conductivity and the specific heat capacity, we consider the following cases:

Case I: $c_1 = 0,\ c_2 = 0,\ \kappa_1 = 0$ (linear heat conduction).
Case II: $c_1 = 0,\ c_2 = 0,\ \kappa_1 = -0.19 \times 10^{-3}$ W/(m K^2).
Case III: $c_1 = 4.5$ J/(kg K^2), $c_2 = 0,\ \kappa_1 = 0$.
Case IV: $c_1 = 4.5$ J/(kg K^2), $c_2 = 0,\ \kappa_1 = -0.19 \times 10^{-3}$ W/(m K^2).

All other parameters (such as ρ, c_0, κ_0. μ and T_0) are as given before for the PMMA solid. For all the four cases, the temperature at $r = 0.045$ mm and selected time instants ($t = 1.72$ s, $t = 9.17$ s and $t = 46.44$ s) is plotted against z ($0 < z < 1$ mm) in Figures 5, 6 and 7. At earlier time, such as $t = 1.72$ s, the temperature in each of the cases is quite close to one another. In Figures 5 and 6, the temperature in Case I is almost visually indistinguishable from that in Case II. Similarly, at earlier time, there is only a very small difference between the temperature in Case III and that in Case IV. This is perhaps not surprising as the value of κ_1 in Cases II and IV is relatively small, close to zero. Nevertheless, as time evolves, the difference in the temperature in each of the cases becomes more pronounced, as is obvious in Figure 7 where the temperature plots for $t = 46.44$ s are given. Each of the temperature-dependent terms in the thermal conductivity and

the specific heat capacity in the PMMA cylindrical solid apparently has the effect of slowing down the heating of the solid.

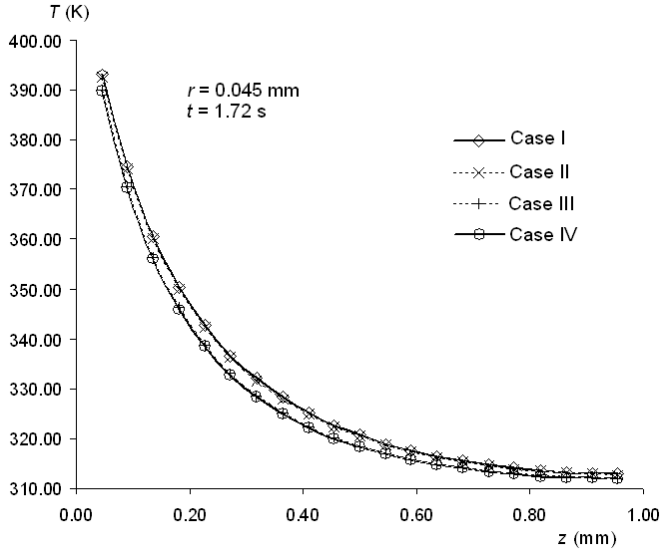

Figure 5. Plots of temperature at $r = 0.045$ mm and time $t = 1.72$ s against z.

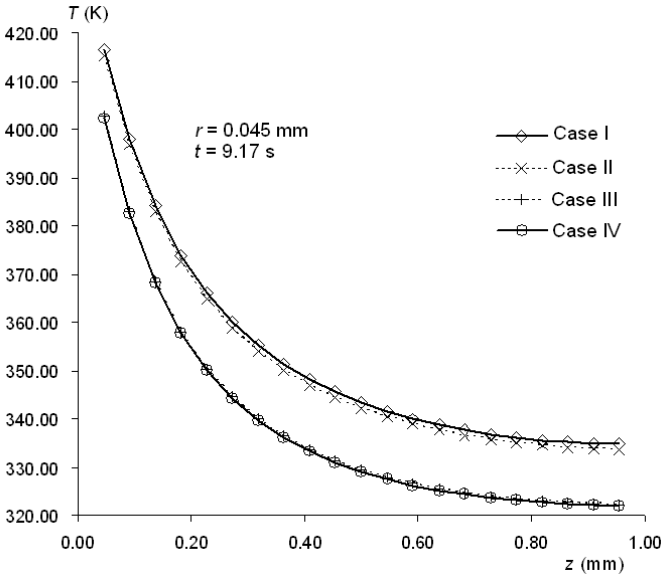

Figure 6. Plots of temperature at $r = 0.045$ mm and time $t = 9.17$ s against z.

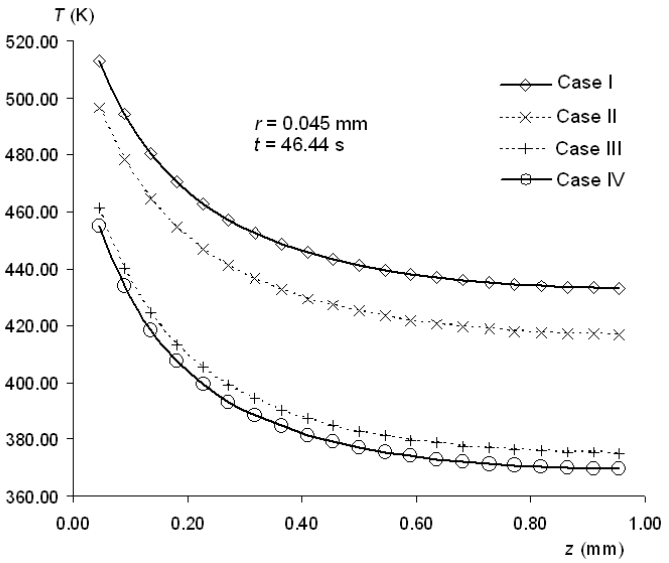

Figure 7. Plots of temperature at $r = 0.045$ mm and time $t = 46.44$ s against z.

7 Summary

The numerical solution of an axisymmetric heat conduction problem involving a nonhomogeneous solid with temperature-dependent properties is considered. Through the use of Kirchhoff's transformation and an appropriate substitution of variables, the problem is formulated in terms of a nonlinear integro-differential equation. The integro-differential equation contains an integral over a curve and a domain integral. The first order time derivative of the temperature is present in the integrand of the domain integral. With the time derivative of the temperature approximated by a finite-difference formula, the line and domain integrals are treated using a dual-reciprocity boundary element procedure. We have proposed a relatively simple interpolating function for use in the dual-reciprocity approximation of the domain integral. The integro-differential equation is eventually reduced to nonlinear algebraic equations which are solved iteratively at consecutive time levels.

To assess the validity and accuracy of the proposed numerical procedure, some problems which have known solutions are solved. The numerical results

agree favorably with the known solutions, indicating that the dual-reciprocity boundary element method together with the proposed interpolating function can be used to provide reliable and accurate numerical solutions for the nonlinear axisymmetric heat equation. Lastly, the method is applied to study the effects of temperature-dependent material properties on the laser heating of a cylindrical solid.

References

[1] M. Abramowitz and I. Stegun, *Handbook of Mathematical Functions*, Dover, New York, 1970.

[2] W. T. Ang and D. L. Clements, Nonlinear heat equation for nonhomogeneous anisotropic materials: a dual-reciprocity boundary element solution. *Numerical Methods for Partial Differential Equations* **26** (2010) 771-784.

[3] W. T. Ang, J. Kusuma and D. L. Clements, A boundary element method for a second order elliptic partial differential equation with variable coefficients. *Engineering Analysis with Boundary Elements* **18** (1996) 311-316.

[4] W. T. Ang and E. H. Ooi, A dual-reciprocity boundary element approach for solving axisymmetric heat equation subject to specification of energy. *Engineering Analysis with Boundary Elements* **32** (2008) 210-215.

[5] M. I. Azis and D. L. Clements, Nonlinear transient heat conduction problems for a class of inhomogeneous anisotropic materials by BEM. *Engineering Analysis with Boundary Elements* **32** (2008) 1054-1060.

[6] C. A. Brebbia, J. C. F. Telles and L. C. Wrobel, *Boundary Element Techniques, Theory and Applications in Engineering*, Springer-Verlag, Berlin/Heidelberg, 1984.

[7] D. L. Clements, A boundary integral equation method for the numerical solution of a second order elliptic partial differential equation with vari-

able coefficients. *Journal of the Australian Mathematical Society (Series B)* **22** (1980) 218-228.

[8] D. L. Clements and W. S. Budhi, A boundary element method for the solution of a class of steady-state problems for anisotropic media. *ASME Journal of Heat Transfer* **121** (1999) 462-465.

[9] T. Goto and M. Suzuki, A boundary integral equation method for non-linear heat conduction problems with temperature-dependent material properties. *International Journal of Heat Mass Transfer* **39** (1996) 823-830.

[10] G. Gutierrez and T. C. Jen, Numerical simulation of non-linear heat conduction subjected to a laser source: the effects of variable thermal properties. *International Journal of Heat Mass Transfer* **43** (2000) 2177-2192.

[11] A. J. Kassab and E. Divo, A generalized boundary integral equation for isotropic heat conduction equation with spatially varying thermal conductivity. *Engineering Analysis with Boundary Elements* **18** (1996) 273-286.

[12] M. Kikuta, H. Togoh and M. Tanaka, Boundary element analysis of non-linear transient heat conduction problems. *Computer Methods in Applied Mechanics and Engineering* **62** (1987) 321-329.

[13] E. H. Ooi, W. T. Ang and E. Y. K. Ng, A boundary element model of the human eye undergoing laser thermokeratoplasty. *Computers in Biology and Medicine* **38** (2008) 727-737.

[14] P. W. Partridge, C. A. Brebbia and L. C. Wrobel, *The Dual Reciprocity Boundary Element Method*, Computational Mechanics Publications, London, 1992.

[15] F. Paŕıs and J. Cañas, *Boundary Element Method: Fundamentals and Applications*, Oxford University Press, Oxford, 1997.

[16] Y. S. Park and W. T. Ang, A complex variable boundary element method for an elliptic partial differential equation with variable coefficients. *Communications in Numerical Methods in Engineering* **16** (2000) 697-703.

[17] R. Rangogni, A solution of Darcy's flow with variable permeability by means of B.E.M. and perturbation techniques. *Boundary Elements IX*, Vol. 3, C. A. Brebbia ed. Springer-Verlag, Berlin, 1987.

[18] M. Tanaka, T. Matsumoto, Y. Suda, A dual-reciprocity boundary element method applied to the steady-state heat conduction problem of functionally gradient materials. Presented at *BETEQ 2001-The 2nd International Conference on Boundary Element Techniques,* Rutgers University, USA, 2001.

[19] K. Wang, R. M. M. Mattheij and H. G. ter Morsche, Alternative DRM formulations. *Engineering Analysis with Boundary Elements* **27** (2003) 175-181.

[20] E. T. Whittaker and G. N. Watson, *A Course in Modern Analysis*, Cambridge University Press, Cambridge, 1990.